

Spatial Averaging of Time–Frequency Distributions for Signal Recovery in Uniform Linear Arrays

Yimin Zhang, *Member, IEEE*, and Moeness G. Amin, *Senior Member, IEEE*

Abstract—This paper presents a new approach based on spatial time–frequency averaging for separating signals received by a uniform linear antenna array. In this approach, spatial averaging of the time–frequency distributions (TFDs) of the sensor data is performed at multiple time–frequency points. This averaging restores the diagonal structure of the source TFD matrix necessary for source separation. With spatial averaging, crossterms move from their off-diagonal positions in the source TFD matrix to become part of the matrix diagonal entries. It is shown that the proposed approach yields improved performance over the case when no spatial averaging is performed. Further, we demonstrate that in the context of source separation, the spatially averaged Wigner–Ville distribution outperforms the combined spatial–time–frequency averaged distributions, such as the one obtained by using the Choi–Williams distribution. Simulation examples involving the separation of two sources with close AM and FM modulations are presented.

Index Terms—Array signal processing, spatial time–frequency distribution, subspace analysis, time–frequency distribution, time–frequency MUSIC.

I. INTRODUCTION

RECENTLY, time–frequency distributions (TFDs) have been employed for direction finding and blind source separation problems in sensor array processing [1]–[5]. The spatial time–frequency distributions (STFDs) were introduced in [1] and represented by a spatial matrix whose elements are the auto- and cross-time–frequency distributions of the data received at the different array sensors. STFD techniques are most appropriate to handle sources of nonstationary waveforms that are localized in the time–frequency domain. The robustness of the subspace estimates using STFD matrices is analyzed in [17] and shown to have an advantage over those obtained from the covariance matrices.

The application of STFDs to separating sources with distinct time–frequency signatures is presented in [2]. In this reference, it is shown that the source TFD matrix, whose elements are the auto- and cross-TFD of the source signals, and the sensor data STFD have the same relationship as the one between the source and the data correlation matrices. This relationship is defined by the mixing or the array manifold matrix. The steps applied in blind source separation based on second-order statistics

(the SOBI technique) outlined in [9] could therefore be used in the time–frequency formulation of the problem. The general theory of solving blind source separation problems using spatial arbitrary joint-variable distributions, including those of time and frequency, is given in [3]. In [4], the two arbitrary variables are chosen as the time-lag and frequency-lag, and the source separation was performed using spatial ambiguity functions. The use of STFDs for direction finding is discussed in [5] and [18], where the time–frequency MUSIC and the time–frequency maximum likelihood techniques are proposed.

Although blind source separations based on TFD outperform the SOBI method for nonstationary signals, the fundamental problem with the bilinear time–frequency approach remains the need for the incorporation of STFD matrices computed only at the source autoterm points. Crossterms impede performance, as they reside on the off-diagonal elements of the source TFD matrix, and as such, violate its diagonal structure necessary for source separation. Identification of autoterm regions are often difficult for a large class of multicomponent nonstationary signals, and even if properly identified, due to the complexity of the impinging signal time–frequency signatures and the use of finite data records, autoterm regions cannot be entirely free from crossterm mainlobe or/and sidelobe contamination.

In this paper, we discuss the role of TFD crossterms and demonstrate the effect of spatial averaging on STFDs. By utilizing the Vandermonde structure of the array manifold matrix and performing spatial averaging on the spatial time–frequency distribution matrices, we set the off-diagonal elements of the corresponding source TFD matrix to zero. This is achieved by moving the crossterms from their off-diagonal positions to join the autoterms as diagonal entries of the source TFD matrix at one time–frequency point. In this respect, the performance of the source separation technique becomes much less dependent on the selection of the time–frequency points at which the STFD matrices are computed. It is shown that the spatially averaged STFDs outperform the case where no spatial averaging is performed, even when only autoterm points are involved in both cases.

Spatial averaging is a simple and well-known technique in conventional array processing [6]. It employs additional array sensors to reduce cross-correlation in coherent and correlated signal environments, thereby permitting proper angle-of-arrival (AOA) estimations and source separations. In this paper, we show that spatial averaging plays a key role in the underlying TFD-based source separation problem, and its application leads to matrix diagonalization and crossterm mitigation. Spatial averaging gives robustness to time–frequency point selections and yields improved performance over other TFD-based techniques,

Manuscript received March 30, 1999; revised May 12, 2000. This work was supported by Office of Naval Research under Grant N00014-98-1-0176. The associate editor coordinating the review of this paper and approving it for publication was Dr. Paulo J. S. G. Ferreira.

The authors are with the Department of Electrical and Computer Engineering, Villanova University, Villanova, PA 19085 USA (e-mail: yimin@ieee.org; moeness@ece.vill.edu).

Publisher Item Identifier S 1053-587X(00)07637-6.

specifically for sources whose signatures are closely separated in the time–frequency domain.

The restoration of the diagonal structure of the source TFD is only part of the problem. Source separation using spatially averaged TFD evaluated at a single time–frequency point can still lead to noisy and nonunique results. Since the power distribution of the signals impinging on the array varies over the time–frequency plane, then different time–frequency points may exhibit different SNR’s. The main two advantages of incorporating several spatially averaged TFD matrices evaluated at different time–frequency points into a joint-diagonalization scheme are to avoid having degenerate eigenvalues and to reduce the possibility of choosing a point with high noise contamination.

It is noted that unlike the method in [2], the proposed approach requires the information on the array manifold and is sensitive to the calibration error. In this case, conventional AOA estimation methods, such as the maximum likelihood [11], matrix pencil [12], MUSIC [13], root MUSIC [14], [15], and ESPRIT [16] techniques can also be used to estimate the mixing matrix and further to separate the source signals. The proposed approach not only requires no angular search but also enjoys the discriminatory property of TFD-based array processing, where fewer sources can be considered by only selecting their respective time–frequency signatures [17]–[19].

This paper is organized as follows. In Section II, the source separation approach based on spatial time–frequency distribution is briefly summarized. In Section III, we introduce the spatially averaged time–frequency distributions and discuss the difference between spatial averaging and kernel methods in handling the crossterm problem. Simulation results demonstrating the usefulness of the proposed technique are given in Section IV.

II. SOURCE SEPARATION BASED ON SPATIAL TIME-FREQUENCY DISTRIBUTIONS

A. Spatial Time–Frequency Distributions

In many practical situations, the data vector $\mathbf{x}(t)$ for an N -element array follows an instantaneous mixture model and is given by

$$\mathbf{x}(t) = \mathbf{y}(t) + \mathbf{n}(t) = \mathbf{A}\mathbf{s}(t) + \mathbf{n}(t) \quad (1)$$

where $\mathbf{x}(t) = [x_0(t), \dots, x_{N-1}(t)]^T$ is the data snapshot vector at time t , and the superscript T denotes transpose. The vector $\mathbf{s}(t) = [s_1(t), \dots, s_n(t)]^T$ contains n source signals at the same time, and $\mathbf{n}(t)$ is the additive noise vector. This model is commonly used in the field of narrowband array processing. The vector $\mathbf{y}(t) = [y_0(t), \dots, y_{N-1}(t)]^T$ contains the noise-free array output. The mixing matrix \mathbf{A} is the transfer function between the source signals and the data at the array sensors. We assume that the mixing matrix \mathbf{A} is full column rank.

The source signal vector $\mathbf{s}(t)$ is assumed to be a deterministic signal vector with correlation matrix

$$\mathbf{R}_{ss}(\tau) = \lim_{T \rightarrow \infty} \frac{1}{T} \sum_{t=1}^T \mathbf{s}(t+\tau)\mathbf{s}^H(t) \quad (2)$$

where superscript H denotes the conjugate transpose of a matrix or a vector. In [2], it is assumed that $\mathbf{R}_{ss}(\tau) = \text{diag}[r_{11}(\tau), \dots, r_{nn}(\tau)]$, where $\text{diag}[\cdot]$ is the diagonal matrix formed with the elements of its vector valued argument, and $r_{ii}(\tau) = \lim_{T \rightarrow \infty} \frac{1}{T} \sum_{t=1}^T s_i(t+\tau)s_i^*(t)$ denotes the correlation of $s_i(t)$. This assumption implies that the components $s_i(t)$, $1 \leq i \leq n$ are mutually uncorrelated. However, in our proposed method, this assumption is no longer necessary.

The additive noise $\mathbf{n}(t)$ is modeled as a stationary, temporally white, zero-mean complex random process independent of the source signals. For simplicity, we also require $\mathbf{n}(t)$ to be spatially white, i.e.,

$$E[\mathbf{n}(t+\tau)\mathbf{n}^H(t)] = \sigma_n^2 \delta(\tau) \mathbf{I} \quad (3)$$

where $\delta(\tau)$ is the Kronecker delta, and \mathbf{I} denotes the identity matrix. Since the signal power and the signal ordering are indeterminable in source separations [3], we simplify the problem by treating the source signals as if they have unit power. Accordingly

$$\mathbf{R}_{ss}(0) = \mathbf{I} \quad \text{and} \quad \mathbf{R}_{yy} = \lim_{T \rightarrow \infty} \frac{1}{T} \sum_{t=1}^T \mathbf{y}(t)\mathbf{y}^H(t) = \mathbf{A}\mathbf{A}^H. \quad (4)$$

The discrete-time form of Cohen’s class of TFD for signal $x(t)$ is given by [7]

$$D_{xx}(t, f) = \sum_{l=-\infty}^{\infty} \sum_{m=-\infty}^{\infty} \phi(m, l) x(t+m+l) \cdot x^*(t+m-l) e^{-4\pi f l} \quad (5)$$

where t and f represent the time index and the frequency index, respectively. The kernel $\phi(m, l)$ characterizes the TFD and is a function of both the time and lag variables. The cross-TFD of two signals $x_i(t)$ and $x_j(t)$ is defined by [7]

$$D_{x_i x_j}(t, f) = \sum_{l=-\infty}^{\infty} \sum_{m=-\infty}^{\infty} \phi(m, l) x_i(t+m+l) \cdot x_j^*(t+m-l) e^{-4\pi f l}. \quad (6)$$

One possible definition of spatial time–frequency distribution (STFD) is given in [2] and incorporates both equations (5) and (6)

$$\mathbf{D}_{xx}(t, f) = \sum_{l=-\infty}^{\infty} \sum_{m=-\infty}^{\infty} \phi(m, l) \mathbf{x}(t+m+l) \cdot \mathbf{x}^H(t+m-l) e^{-4\pi f l} \quad (7)$$

where $[\mathbf{D}_{xx}(t, f)]_{i,j} = D_{x_i x_j}(t, f)$ for $i, j = 0, \dots, N-1$. It is shown in the next section that other forms of STFD can be more useful in the context of source separation. Under the linear data model of (1), and assuming a noise-free environment, the STFD matrix in (7) takes the following simple structure:

$$\mathbf{D}_{xx} = \mathbf{A}\mathbf{D}_{ss}(t, f)\mathbf{A}^H \quad (8)$$

where $\mathbf{D}_{ss}(t, f)$ is the signal TFD matrix whose entries are the auto- and cross-TFDs of the sources. Equation(8) is similar to the formula that is commonly used in conventional blind source

separation and direction-of-arrival (DOA) estimation problems [8], [9], relating the signal correlation matrix to the data spatial correlation matrix. If $\mathbf{D}_{ss}(t, f)$ is a full-rank matrix, the two subspaces spanned by the principle eigenvectors of $\mathbf{D}_{xx}(t, f)$ and the columns of \mathbf{A} become identical. In this case, direction-finding techniques based on eigenstructures can be applied. If $\mathbf{D}_{ss}(t, f)$ is diagonal, i.e., the signal cross-TFDs at the time-frequency point (t, f) are zeros, the mixture matrix and the signal waveforms can be recovered using blind source separation methods [1], [2].

B. Source Separation Based on Spatial Time-Frequency Distributions

The source separation algorithm based on spatial time-frequency distributions is an essential part of the proposed method. The algorithm is given in details in [2] and is summarized below.

The first step is the whitening of the signal part $\mathbf{y}(t)$ of the observation. This is achieved by applying a whitening matrix \mathbf{W} to $\mathbf{y}(t)$, i.e., an $n \times N$ matrix satisfying

$$\begin{aligned} \lim_{T \rightarrow \infty} \frac{1}{T} \sum_{t=1}^T \mathbf{W} \mathbf{y}(t) \mathbf{y}^H(t) \mathbf{W}^H &= \mathbf{W} \mathbf{R}_{yy} \mathbf{W}^H \\ &= \mathbf{W} \mathbf{A} \mathbf{A}^H \mathbf{W}^H \\ &= \mathbf{I}. \end{aligned} \quad (9)$$

$\mathbf{W} \mathbf{A}$ is an $n \times n$ unitary matrix \mathbf{U} , and matrix \mathbf{A} can be written as

$$\mathbf{A} = \mathbf{W}^{\#} \mathbf{U} \quad (10)$$

where superscript $\#$ denotes pseudo-inverse. The whitened process $\mathbf{z}(t) = \mathbf{W} \mathbf{x}(t)$ still obeys a linear model

$$\mathbf{z}(t) = \mathbf{W} \mathbf{x}(t) = \mathbf{W} [\mathbf{A} \mathbf{s}(t) + \mathbf{n}(t)] = \mathbf{U} \mathbf{s}(t) + \mathbf{W} \mathbf{n}(t). \quad (11)$$

By pre- and post-multiplying the STFD matrices $\mathbf{D}_{xx}(t, f)$ by \mathbf{W} , we obtain

$$\mathbf{D}_{zz}(t, f) = \mathbf{W} \mathbf{D}_{xx}(t, f) \mathbf{W}^H \quad (12)$$

which is, in essence, the STFD of the whitened data vector $\mathbf{z}(t)$. From the definitions of \mathbf{W} and \mathbf{U}

$$\mathbf{D}_{zz}(t, f) = \mathbf{U} \mathbf{D}_{ss}(t, f) \mathbf{U}^H. \quad (13)$$

Equation (13) shows that if $\mathbf{D}_{ss}(t, f)$ is diagonal, then any whitened data STFD matrix is diagonal in the basis of the columns of the matrix \mathbf{U} , and the eigenvalues of $\mathbf{D}_{zz}(t, f)$ are the diagonal entries of $\mathbf{D}_{ss}(t, f)$. An estimate $\hat{\mathbf{U}}$ of the unitary matrix \mathbf{U} may be obtained as a signal subspace of a whitened STFD matrix evaluated at a time-frequency point corresponding to the signal autoterm. The source signals can then be estimated as $\hat{\mathbf{s}}(t) = \hat{\mathbf{U}} \hat{\mathbf{W}} \mathbf{x}(t)$, and the mixing matrix \mathbf{A} is estimated by $\hat{\mathbf{A}} = \hat{\mathbf{W}}^{\#} \hat{\mathbf{U}}$.

Although the unitary matrix can be obtained from a single time-frequency point, STFDs corresponding to different (t, f) points should be incorporated to reduce the possibility of having degenerate eigenvalues and, subsequently, nonunique solutions. The joint-diagonalization (JD) scheme can be used to incorporate multiple time-frequency points [2]. This scheme

forms K STFD matrices $\{\mathbf{D}_{zz}(t_i, f_i) | i = 1, \dots, K\}$ at a set of preferable K time-frequency autoterm points. The unitary matrix $\hat{\mathbf{U}}$ is then obtained as the joint diagonalizer of the set $\{\mathbf{D}_{zz}(t_i, f_i) | i = 1, \dots, K\}$.

III. SPATIAL AVERAGING TIME-FREQUENCY DISTRIBUTIONS

A. Spatial Averaging Methods

The spatial averaging method was introduced by Pillai [6] to restore the full-rank property of the signal correlation matrix in the presence of coherent signals. Unlike other spatial smoothing methods [20]–[23], which only restore the full-rank property of the mixing matrix when the impinging signals are coherent, the spatial averaging method enforces the diagonal structure of the signal correlation matrix. This diagonal matrix property is essential to perform source separation, as previously discussed. Here, we present the role of spatial averaging in the context of TFD analysis and propose signal separation using joint diagonalization based on spatial averaging of spatial TFD matrices.

The basic idea of spatial averaging is to use subarrays of a uniform linear array to obtain an averaged correlation matrix or, in the underlying problem, an averaged STFD matrix, with the off-diagonal elements set to zero.

Without loss of generality, we consider a simple example of $n = 2$, i.e., there are only two sources $s_1(t)$ and $s_2(t)$. The result is generally true for n sources and N sensors, as long as $n < N$.

By ignoring the effect of noise, the received signal at the i th array sensor ($i = 0, 1, \dots, N - 1$) is represented by

$$x_i(t) = x_i^{(1)}(t) + x_i^{(2)}(t) = s_1(t) e^{-j d_i \omega_1} + s_2(t) e^{-j d_i \omega_2} \quad (14)$$

where $\omega_k = 2\pi \sin \phi_k / \lambda$, $k = 1, 2$ are the spatial radian frequencies, ϕ_k are the angles-of-arrival, λ is the RF wavelength, and d_i is the distance between the zeroth and the i th array sensors. The cross-TFD of $x_i(t)$ and $x_j(t)$, assuming uniform linear array, is

$$\begin{aligned} D_{x_i x_j}(t, f) &= D_{x_i^{(1)} x_j^{(1)}}(t, f) + D_{x_i^{(2)} x_j^{(1)}}(t, f) \\ &\quad + D_{x_i^{(2)} x_j^{(2)}}(t, f) + D_{x_i^{(1)} x_j^{(2)}}(t, f) \\ &= \left[D_{s_1 s_1}(t, f) + D_{s_2 s_1}(t, f) e^{-j d_i (\omega_2 - \omega_1)} \right] \\ &\quad \cdot e^{-j (d_i - d_j) \omega_1} \\ &\quad + \left[D_{s_2 s_2}(t, f) + D_{s_1 s_2}(t, f) e^{-j d_i (\omega_2 - \omega_1)} \right] \\ &\quad \cdot e^{-j (d_i - d_j) \omega_2}. \end{aligned} \quad (15)$$

Due to the presence of the cross-terms [second term in each bracket in (15)], the TFD matrix $\mathbf{D}_{xx}(t, f)$ does not provide the proper information to carry out source separations.

The auto- and cross-TFD of the data $x_0(t)$ and $x_i(t)$, $i = 0, 1, \dots, N - 1$ is

$$\begin{aligned} D_{x_0 x_i}(t, f) &= [D_{s_1 s_1}(t, f) + D_{s_2 s_1}(t, f)] e^{j d_i \omega_1} \\ &\quad + [D_{s_2 s_2}(t, f) + D_{s_1 s_2}(t, f)] e^{j d_i \omega_2} \end{aligned} \quad (16)$$

where we used the sensor receiving $x_0(t)$ as the reference sensor and set $d_0 = 0$. Denote $b_1(t, f) = D_{s_1 s_1}(t, f) + D_{s_2 s_1}(t, f)$ and $b_2(t, f) = D_{s_2 s_2}(t, f) + D_{s_1 s_2}(t, f)$. The values of $b_1(t, f)$ and $b_2(t, f)$ are generally complex. If $b_1(t, f)$ and

$b_2(t, f)$ are real, then the Hermitian Toeplitz spatial time–frequency matrix

$$\bar{D}_{\mathbf{x}\mathbf{x}}(t, f) = \begin{bmatrix} D_{x_0x_0}(t, f) & D_{x_0x_1}(t, f) & \cdots & D_{x_0x_{N-1}}(t, f) \\ D_{x_0x_1}^*(t, f) & D_{x_0x_0}(t, f) & \cdots & D_{x_0x_{N-2}}(t, f) \\ \vdots & \vdots & \ddots & \vdots \\ D_{x_0x_{N-1}}^*(t, f) & D_{x_0x_{N-2}}^*(t, f) & \cdots & D_{x_0x_0}(t, f) \end{bmatrix} \quad (17)$$

generated from the cross-TFDs $D_{x_0x_0}(t, f)$, $D_{x_0x_1}(t, f)$, \dots , $D_{x_0x_{N-1}}(t, f)$ between the data samples at the reference sensor and those at other sensors of the array can be expressed as [24]

$$\bar{D}_{\mathbf{x}\mathbf{x}}(t, f) = \mathbf{A}\bar{D}_{\mathbf{s}\mathbf{s}}(t, f)\mathbf{A}^H \quad (18)$$

where \mathbf{A} is a Vandermonde matrix, and

$$\bar{D}_{\mathbf{s}\mathbf{s}}(t, f) = \text{diag}[b_1(t, f), b_2(t, f)] \quad (19)$$

is the corresponding source TFD matrix. Note that $\bar{D}_{\mathbf{x}\mathbf{x}}(t, f)$ has a different structure from that of the STFD matrix defined in (7) and was used in [2] for blind source separation. Clearly, (18) has the same form as (8), but $\bar{D}_{\mathbf{s}\mathbf{s}}(t, f)$ here is diagonal, even if the selected (t, f) point corresponds to a crossterm.

In the case of complex signal waveforms, the realness and the diagonal structure of $\bar{D}_{\mathbf{s}\mathbf{s}}(t, f)$ can be restored by spatial averaging. We add $N - 1$ array sensors symmetrically about the reference point, as shown in Fig. 1. The received signal at i th sensor of the new set is

$$x_{-i}(t) = x_{-i}^{(1)}(t) + x_{-i}^{(2)}(t) = s_1(t)e^{jd_i\omega_1} + s_2(t)e^{jd_i\omega_2}. \quad (20)$$

The new cross-TFD of $x_0(t)$ and $x_{-i}(t)$ is

$$D_{x_0x_{-i}}(t, f) = [D_{s_1s_1}(t, f) + D_{s_2s_1}(t, f)]e^{-jd_i\omega_1} + [D_{s_2s_2}(t, f) + D_{s_1s_2}(t, f)]e^{-jd_i\omega_2}. \quad (21)$$

The spatial averaging of (16) and (21) is given by

$$\begin{aligned} \tilde{D}_{xx}^{(i)}(t, f) &= [D_{x_0x_i}(t, f) + D_{x_0x_{-i}}^*(t, f)]/2 \\ &= c_1(t, f)e^{jd_i\omega_1} + c_2(t, f)e^{jd_i\omega_2} \end{aligned} \quad (22)$$

where

$$\begin{aligned} c_1(t, f) &= D_{s_1s_1}(t, f) + \text{Re}[D_{s_2s_1}(t, f)] \\ c_2(t, f) &= D_{s_2s_2}(t, f) + \text{Re}[D_{s_1s_2}(t, f)]. \end{aligned}$$

Since the terms in the brackets in (21) are all real, the matrix formed from the TFDs (22)

$$\tilde{D}_{\mathbf{x}\mathbf{x}}(t, f) = \begin{bmatrix} \tilde{D}_{xx}^{(0)}(t, f) & \tilde{D}_{xx}^{(1)}(t, f) & \cdots & \tilde{D}_{xx}^{(N-1)}(t, f) \\ \tilde{D}_{xx}^{(1)*}(t, f) & \tilde{D}_{xx}^{(0)}(t, f) & \cdots & \tilde{D}_{xx}^{(N-2)}(t, f) \\ \vdots & \vdots & \ddots & \vdots \\ \tilde{D}_{xx}^{(N-1)*}(t, f) & \tilde{D}_{xx}^{(N-2)*}(t, f) & \cdots & \tilde{D}_{xx}^{(0)}(t, f) \end{bmatrix} \quad (23)$$

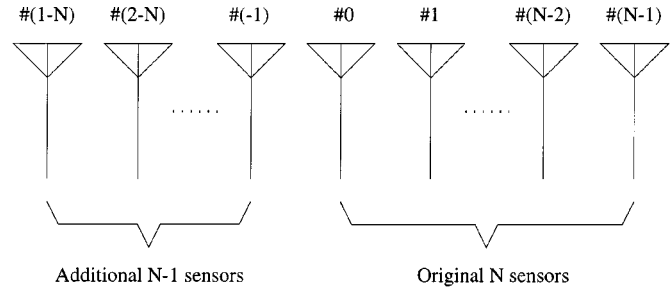


Fig. 1. Array configuration for spatial averaging.

is Hermitian and Toeplitz. This matrix is referred to as the spatially averaged TFD (SATFD) matrix. Similar to the real TFD case, in the noise-free environment, the SATFD matrix in (23) can be expressed as

$$\tilde{D}_{\mathbf{x}\mathbf{x}}(t, f) = \mathbf{A}\tilde{D}_{\mathbf{s}\mathbf{s}}(t, f)\mathbf{A}^H \quad (24)$$

where

$$\tilde{D}_{\mathbf{s}\mathbf{s}}(t, f) = \text{diag}[c_1(t, f), c_2(t, f)]. \quad (25)$$

The off-diagonal elements of $\tilde{D}_{\mathbf{s}\mathbf{s}}(t, f)$ are zero, whereas the matrix diagonal entries are now made up of both autoterms and crossterms of the impinging source signals. By enforcing the diagonal structure of the source TFD matrix $\tilde{D}_{\mathbf{s}\mathbf{s}}(t, f)$, spatial averaging of the Hermitian Toeplitz STFD matrices extends the validity of the TFD-based signal separation in the presence of cross-TFDs.

The steps for source separation used in [2] and summarized in Section II can be applied to the SATFD $\tilde{D}_{\mathbf{x}\mathbf{x}}(t, f)$ instead of the STFD $D_{\mathbf{x}\mathbf{x}}(t, f)$. With spatial averaging, the incorporation of STFDs at only autoterm points into the joint-diagonalization scheme is no longer crucial to achieve good performance.

B. Comparison between Spatial Averaging and Kernel Methods

There are two sources of crossterms in the underlying source separation problem. The first type are the crossterms that are the results of the interactions between the components of the same source signal. Whether we use the STFD defined in (7) or in (17), those crossterms are not harmful to the blind source separation problem since they always reside, along with the autoterms, on the main diagonal of the source TFD matrix. The other type of crossterms are those generated from the interactions between two signal components belonging to two different sources. These crossterms are associated with cross-TFDs of the source signals, and at any given time–frequency point, they constitute the off-diagonal entries of the source TFD matrices. The crossterms generated from the data cross-TFDs violate the basic assumption in the problem of source separation regarding the diagonal structure of the source TFD matrix. We must therefore select the time–frequency points that belong to autoterm regions where crossterm contributions are at minimum. However, the selection of autoterm points is often difficult in the absence of *a priori* information of the source signals, specifically for low SNR or when the signals have highly overlapping time–frequency signatures. The later case can be encountered in radar echoes and acoustic signal processing.

The use of smoothing time–frequency kernel for crossterm reduction is a candidate solution of the above problem. The main function of this kernel in the context of source separation is to prevent the selection and incorporation of crossterm points in the joint-diagonalization scheme, as well as to reduce the contribution of crossterms at selected autoterm points. In essence, the fundamental role of the time–frequency kernel is to make the source TFD matrices as close to a diagonal structure as possible. The time–frequency kernel can be applied to both forms of STFDs in (7) and (23). It is noteworthy that the smoothing kernel does not distinguish between the aforementioned two types of crossterms, and accordingly, it reduces all entries of the source TFD matrix, including the diagonal elements.

The problem with the smoothing kernel is fourfold. First, for sources with closely separated time–frequency signatures, the effectiveness of the smoothing kernel in reducing crossterms is highly impaired. Second, reduction of crossterms depends on their time–frequency locations, especially when fixed shape kernels are used. For example, time–frequency kernels satisfying the marginal properties are not suitable for removing the crossterms which lie on the time-lag and frequency-lag axes in the ambiguity domain. Third, depending on the employed time–frequency kernel, part or all of the crossterms may be displaced to mount on the selected autoterm points. The situation can make the source TFD matrix further deviate from a diagonal structure and cause performance deterioration from the case when no smoothing is applied. We refer to this undesired property as the smoothing problem. Fourth, since source separation is often performed incorporating a finite number of data samples, the intrusion of crossterms on autoterm regions cannot be prevented or entirely removed. This is because the window spreads out the crossterms in the time–frequency domain so that the mainlobe or/and the sidelobes of the crossterms are deemed to overlap with the signal autoterms. We refer to this undesired property as the leakage problem in STFDs. In addition to the above drawbacks, the time–frequency kernel ignores the fact that the first type of crossterms need not be smoothed, as its appearance along the diagonal elements can improve the effective signal-to-noise ratio.

The spatial averaging of the STFD defined in (23) at a given (t, f) point does not smooth or reduce the crossterms at that point but rather moves them from their residence on the off-diagonal matrix entries to be part of the matrix diagonal elements. The other part represents the contribution of the autoterms at the same point. Therefore, not only we are able to set the off-diagonal elements of the source TFD matrix to zeros, but we can also improve performance by selecting the (t, f) points of peak values, irrespective of whether these points belong to autoterm or crossterm regions.

IV. PERFORMANCE EVALUATION

A. Performance Index

We use a slightly modified version of the performance index applied in [2] to evaluate the performance of the proposed source separation technique. The estimate of the source signal vector is computed by applying the pseudo-inverse of the

estimated mixing matrix $\hat{\mathbf{A}}$ to the received signal vector $\mathbf{x}(t)$, i.e.,

$$\hat{\mathbf{s}}(t) = \hat{\mathbf{A}}^\# \mathbf{x}(t) = \hat{\mathbf{A}}^\# \mathbf{A}\mathbf{s}(t) + \hat{\mathbf{A}}^\# \mathbf{n}(t) \quad (26)$$

where $\hat{\mathbf{A}} = \hat{\mathbf{W}}^\# \hat{\mathbf{U}}$. We stress that in general, this procedure is not optimal for recovering the source signals based on an estimate $\hat{\mathbf{A}}$. For large enough sample size, matrix $\hat{\mathbf{A}}$ should be close to the true one \mathbf{A} so that $\hat{\mathbf{A}}^\# \mathbf{A}$ well approximates the identity matrix. We normalize matrix $\hat{\mathbf{A}}$ by

$$\hat{\mathbf{A}}_e = \hat{\mathbf{A}} \text{diagonal}(\hat{\mathbf{A}}^\# \mathbf{A}) \quad (27)$$

where $\text{diagonal}(\mathbf{F})$ denotes the matrix formed by the diagonal elements of \mathbf{F} . As such, the diagonal elements of $\hat{\mathbf{A}}_e^\# \mathbf{A}$ become exactly one, giving more meaning to the performance index

$$I_{pq} = E \left| (\hat{\mathbf{A}}_e^\# \mathbf{A})_{pq} \right|^2 \quad (28)$$

which defines the interference-to-signal ratio (ISR). Thus, I_{pq} measures the ratio of the power of the interference of q th source signal to the power of the p th source signal. As the measure of the global quality of the separation process, we also apply the global rejection level to evaluate the overall performance of the proposed method

$$I_{perf} = \sum_{q \neq p} I_{pq} \quad (29)$$

B. Effect of Crossterms between Source Signals

In this section, we examine the effect of the time–frequency crossterms on source separation performance when spatial averaging is not applied. To simplify the problem, we assume that \mathbf{R}_{ss} is an identity matrix. When crossterms are present at the off-diagonal elements of the TFD matrix $\mathbf{D}_{ss}(t, f)$, then

$$\mathbf{D}_{ss}(t, f) = \mathbf{P}(t, f) \mathbf{G}(t, f) \mathbf{P}^H(t, f) \quad (30)$$

where $\mathbf{G}(t, f)$ is the diagonal matrix with the eigenvalues at the diagonal elements, and $\mathbf{P}(t, f)$ is the matrix whose columns are the corresponding eigenvectors. Note that all the above matrices depend on the selected (t, f) point. Substituting (30) in (8), the STFD matrix of the data vector under noise-free conditions becomes

$$\begin{aligned} \mathbf{D}_{xx}(t, f) &= \mathbf{A} \mathbf{D}_{ss}(t, f) \mathbf{A}^H \\ &= \mathbf{A} \mathbf{P}(t, f) \mathbf{G}(t, f) \mathbf{P}^H(t, f) \mathbf{A}^H \end{aligned} \quad (31)$$

and the STFD matrix of the whitened array signal vector is

$$\begin{aligned} \mathbf{D}_{zz}(t, f) &= \mathbf{W} \mathbf{A} \mathbf{D}_{ss}(t, f) \mathbf{A}^H \mathbf{W}^H \\ &= \mathbf{W} \mathbf{A} \mathbf{P}(t, f) \mathbf{G}(t, f) \mathbf{P}^H(t, f) \mathbf{A}^H \mathbf{W}^H. \end{aligned} \quad (32)$$

Since $\mathbf{G}(t, f)$ is diagonal, $\mathbf{W} \mathbf{A} \mathbf{P}(t, f)$ is unitary. If the estimated mixing matrix $\hat{\mathbf{A}}$ is provided based on a single (t, f) point, then from (32)

$$\hat{\mathbf{A}} = \mathbf{W}^\# \mathbf{W} \mathbf{A} \mathbf{P}(t, f) = \mathbf{A} \mathbf{P}(t, f) \quad (33)$$

which is dependent on the unitary matrix $\mathbf{P}(t, f)$. Furthermore

$$\hat{\mathbf{A}}^\# \mathbf{A} = [\mathbf{A}\mathbf{P}(t, f)]^\# \mathbf{A} = \mathbf{P}^H(t, f) \quad (34)$$

and

$$\begin{aligned} \hat{\mathbf{A}}_e^\# \mathbf{A} &= [\text{diagonal}(\hat{\mathbf{A}}^\# \mathbf{A})]^{-1} \hat{\mathbf{A}}^\# \mathbf{A} \\ &= [\text{diagonal}(\mathbf{P}^H(t, f))]^{-1} \mathbf{P}^H(t, f) \\ &= \begin{bmatrix} p_{11}^{-1}(t, f) & & & \mathbf{O} \\ & p_{22}^{-1}(t, f) & & \\ & & \ddots & \\ \mathbf{O} & & & p_{nn}^{-1}(t, f) \end{bmatrix}^* \\ &\quad \cdot \begin{bmatrix} p_{11}(t, f) & p_{21}(t, f) & \cdots & p_{n1}(t, f) \\ p_{12}(t, f) & p_{22}(t, f) & \cdots & p_{n2}(t, f) \\ \vdots & \vdots & \ddots & \vdots \\ p_{1n}(t, f) & p_{2n}(t, f) & \cdots & p_{nn}(t, f) \end{bmatrix}^* \\ &= \begin{bmatrix} 1 & p_{22}^{-1}p_{21}(t, f) & \cdots & p_{nn}^{-1}p_{n1}(t, f) \\ p_{11}^{-1}p_{12}(t, f) & 1 & \cdots & p_{nn}^{-1}p_{n2}(t, f) \\ \vdots & \vdots & \ddots & \vdots \\ p_{11}^{-1}p_{1n}(t, f) & p_{22}^{-1}p_{2n}(t, f) & \cdots & 1 \end{bmatrix}^* \end{aligned} \quad (35)$$

where $p_{ij} = [\mathbf{P}(t, f)]_{ij}$. Accordingly, the performance index becomes

$$I_{pq} = |p_{qq}^{-1}(t, f)p_{qp}(t, f)|^2 \quad (36)$$

and the global rejection level is given by

$$\begin{aligned} I_{perf} &= \sum_{q \neq q} I_{pq} \\ &= \sum_{q=1}^n |p_{qq}(t, f)|^{-2} \sum_{p=1, p \neq q}^n |p_{qp}(t, f)|^2 \\ &= \sum_{q=1}^n |p_{qq}(t, f)|^{-2} - n. \end{aligned} \quad (37)$$

In general, since the absolute values of $p_{qq}(t, f)$ are always equal to or smaller than 1, the global rejection level I_{perf} takes a positive value. It is clear that $I_{perf} = 0$ only when $p_{qq}(t, f) = 1$ holds true for all q . That is, \mathbf{P} is an identity matrix, which implies that there is no off-diagonal nonzero elements in matrix $\mathbf{D}_{ss}(t, f)$.

Consider the specific case of $n = 2$. If we select a (t, f) point where the contributions of the two sources to the source TFD matrix are the same, i.e., $D_{s_1 s_1}(t, f) = D_{s_2 s_2}(t, f)$, and since $D_{s_1 s_2}(t, f) = D_{s_2 s_1}^*(t, f)$ by definition, then it is straightforward to show that $|p_{qq}(t, f)| = 1/\sqrt{2}$. In this case, I_{perf} is constant equal to 2. The (t, f) points having such property include all crossterms at which the autoterms have equal contributions.

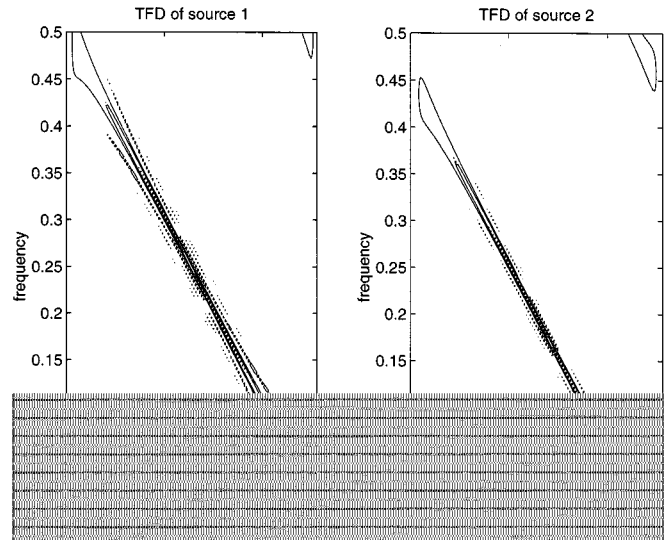


Fig. 2. TFD of the source signals (Wigner-Ville distribution).

C. Simulation Results

In this section, we demonstrate the effectiveness of the spatially averaged time-frequency distributions in source separations. The whitening joint-diagonalization scheme [2] is used for incorporating multiple time-frequency points into the proposed spatial averaging method. In all simulations, two sources with the chirp signals

$$s_1(t) = e^{-j\mu(t^2/2)}, \quad s_2(t) = e^{-j\mu(t^2/2) - (\alpha + j\omega)t} \quad (38)$$

are used, where μ is chosen as 0.008π . Different values of ω and α are considered. These values control the frequency offset and amplitude variation between the two signals and can be chosen to yield closely or widely separated source signatures in the time-frequency domain. We consider 128 data samples from which a time-frequency matrix of 128×128 is formed. The DOAs of the two signals $s_1(t)$ and $s_2(t)$ are set equal to 30° and 60° , respectively, from the broadside direction. Furthermore, we assume an equispaced five-element linear array with the interelement spacing 0.5λ , where λ is the wavelength. Subsequently, when the spatial averaging method is used, two subarrays are formed, each with three elements.

In the first set of simulations, we choose $\alpha = 0$, i.e., neither signal is amplitude modulated. The Wigner-Ville (WV) distribution of each signal is shown in Fig. 2, where $\delta f (= \omega/2\pi)$ is set equal to 0.05. Fig. 3 shows the time-frequency distribution of the mixed signals at the center array sensor. No noise is present for this case. It is clear that the crossterms lie in the middle of the two chirps, and their amplitude changes periodically. Fig. 4(a) shows the time-frequency distributions of the separated signals using the technique in [2], where joint diagonalization is used without the utilization of the proposed spatial averaging method. Three time-frequency (t, f) points are used at $t = 32, 64,$ and 96 . The frequency f is chosen so that the TFD computed using the data at the center array sensor is the largest at each t . Peak values of the WV distribution may either correspond to autoterms or crossterms. In this case, out of three

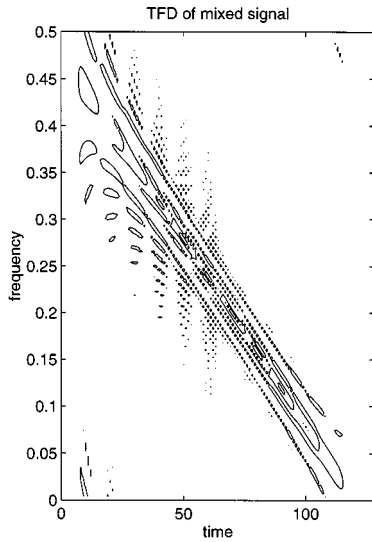


Fig. 3. TFD of the mixed signal (Wigner-Ville distribution).

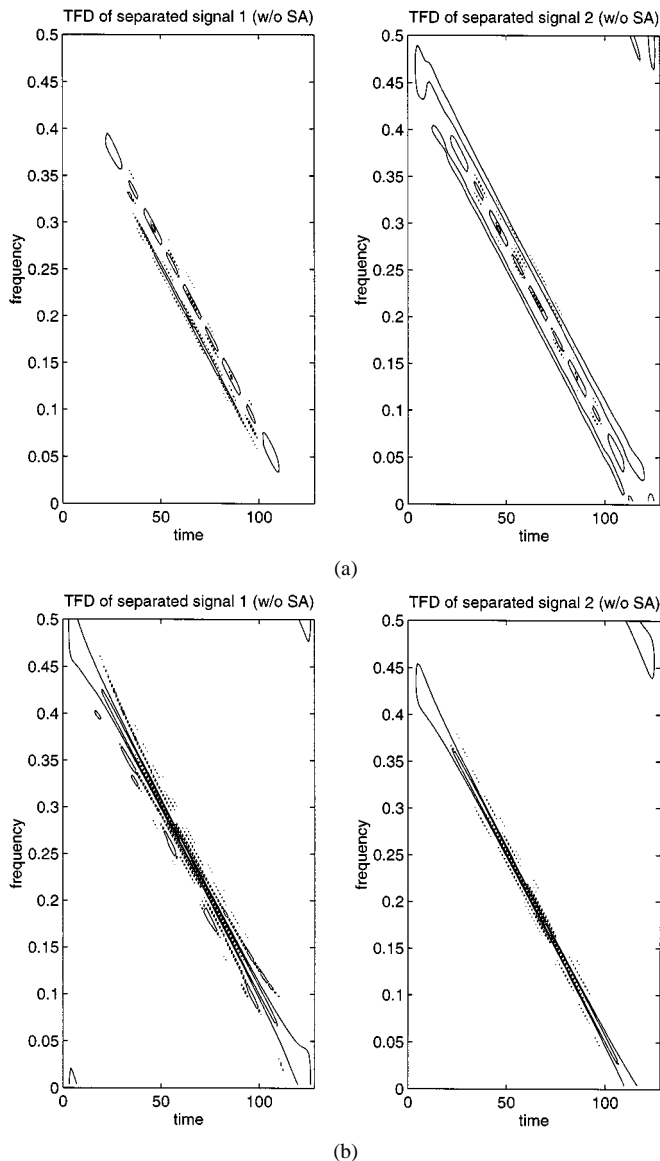


Fig. 4. TFD of the separated signals without spatial averaging (Wigner-Ville distribution). (a) Using peak time-frequency points. (b) Using autoterm points.

(t, f) points, one crossterm point and two autoterm peaks were selected. The obtained $\hat{\mathbf{A}}_e^\# \mathbf{A}$ matrix is

$$\hat{\mathbf{A}}_e^\# \mathbf{A} = \begin{bmatrix} 1.00 + j0.00 & 0.19 + j0.65 \\ -0.21 + j0.63 & 1.00 + j0.00 \end{bmatrix}$$

and the computed global rejection level I_{perf} is -0.43 dB. The result is clearly unsatisfactory, as the matrix $\hat{\mathbf{A}}_e^\# \mathbf{A}$ is far from the identity matrix, and crossterms appear in the separated signals.

Next, we force the selection of autoterm peaks by only considering the (t, f) points along the instantaneous frequencies of the two input signals at the same above time instants. Although no crossterm point is selected, yet as discussed in Section III, because of the finite data record, the crossterms leak into autoterm regions, causing the source TFD matrix to deviate from a diagonal structure. We show in Fig. 4(b) the result of source separation when only the autoterm points are considered. The obtained $\hat{\mathbf{A}}_e^\# \mathbf{A}$ matrix becomes

$$\hat{\mathbf{A}}_e^\# \mathbf{A} = \begin{bmatrix} 1.00 + j0.00 & 0.00 - j0.06 \\ -0.01 - j0.01 & 1.00 + j0.00 \end{bmatrix}$$

and the respective global rejection level I_{perf} is -23.96 dB. It is clear that the source separation performance is greatly improved. This good performance implies that the contributions of crossterms at the three selected autoterm points were insignificant, implying that the corresponding source TFD matrices in this case were close to diagonal.

Fig. 5 shows the time-frequency distributions of the separated signals at the same condition as Fig. 4(a), except with the utilization of the proposed spatial averaging method. Spatial averaging entirely mitigates the effect of crossterms. It is clear that the time-frequency distributions of the separated signals are the same as those of the original source signals, and $\hat{\mathbf{A}}_e^\# \mathbf{A}$ are exactly identity matrices. Similar results can be obtained when all three (t, f) points are autoterms.

Fig. 6 shows the global rejection level I_{perf} versus the frequency difference δf between the two chirps, where the input SNR is 20 dB. When the proposed spatial averaging method is used, the global rejection level maintains low values. On the other hand, without spatial averaging, the global rejection levels become very high. The main reason of the large fluctuation of the I_{perf} without spatial averaging is that the influence as well as the number of crossterm points incorporated in the joint-diagonalization scheme varies with the frequency difference δf (when $\delta f = 0.1$, no crossterm points were selected). Note that the crossterms of the Wigner-Ville distribution remain high even when the frequency difference is large. When selected, these terms put large values along the off-diagonal terms of the source TFD matrix and subsequently cause considerable error, as is evident from the figure. However, when only autoterm (t, f) points are used, the global rejection level decreases as δf increases. In this case, the matrix off-diagonal elements are the crossterm values at the autoterm points that become smaller for higher values of δf .

Next, we show the effect of using time-frequency smoothing kernels for reduced interference terms. The Choi-Williams

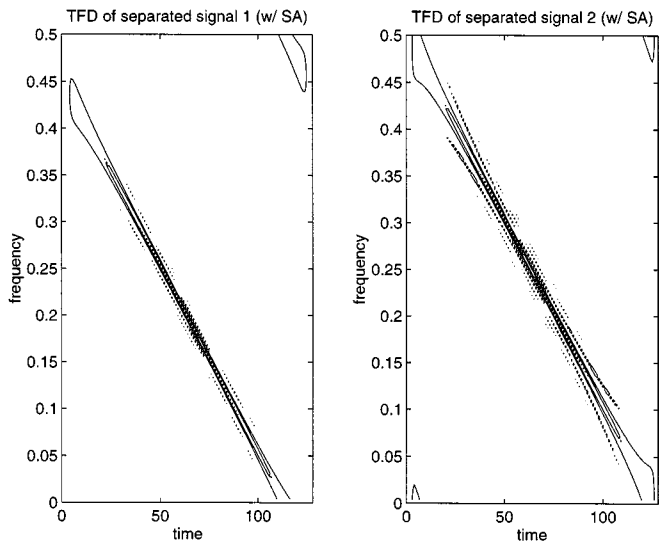


Fig. 5. TFD of the separated signals with spatial averaging (Wigner-Ville distribution).

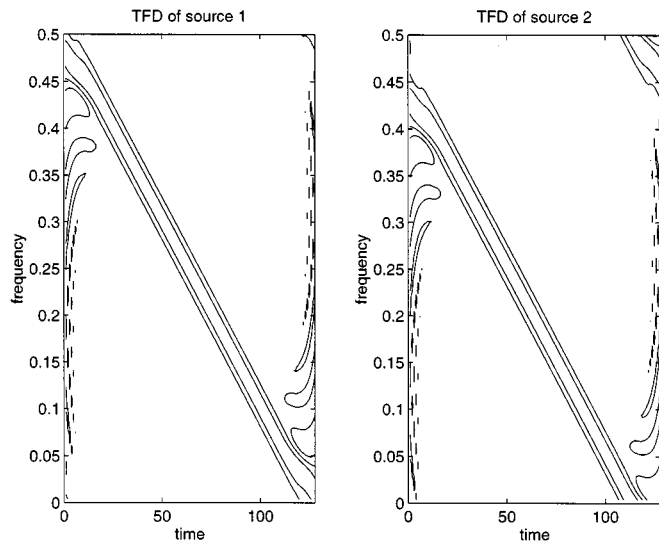


Fig. 7. TFD of the source signals (Choi-Williams distribution).

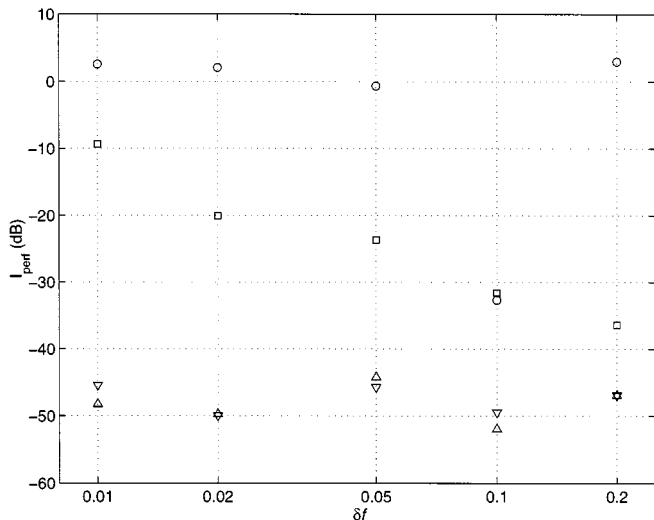


Fig. 6. Global rejection level versus frequency difference δf (Wigner-Ville distribution). (Input SNR = 20 dB; o: without spatial averaging; Δ : with spatial averaging; \square : without spatial averaging using autoterm points; ∇ : with spatial averaging using autoterm points).

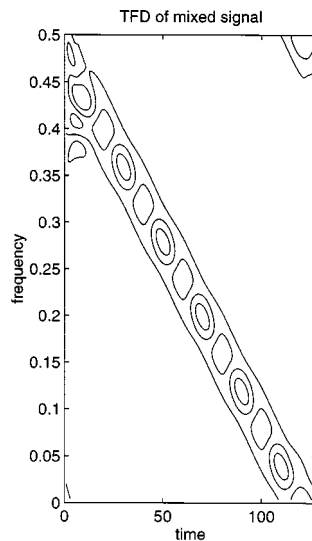


Fig. 8. TFD of the mixed signal (Choi-Williams distribution).

(CW) distribution [10] is considered with $\sigma = 1$. Fig. 7 shows the CW distribution of each signal separately, whereas the CW distribution of the mixed signals at the center array sensor is depicted in Fig. 8. The signals are the same as the ones used in the WV distribution simulations with $\delta f = 0.05$. Fig. 9(a) shows the CW distributions of the separated signals. The obtained $\hat{\mathbf{A}}_e^\# \mathbf{A}$ matrix is

$$\hat{\mathbf{A}}_e^\# \mathbf{A} = \begin{bmatrix} 1.00 + j0.00 & 0.03 + j0.70 \\ -0.05 + j0.67 & 1.00 + j0.00 \end{bmatrix}$$

and the respective global rejection level I_{perf} is -0.26 dB. At this small frequency offset, effective smoothing of crossterms is difficult, and as a result, even with the use of time-frequency kernel, one crossterm (t, f) point was still selected out of the

three (t, f) points. When only the autoterm (t, f) points are used, the $\hat{\mathbf{A}}_e^\# \mathbf{A}$ matrix becomes

$$\hat{\mathbf{A}}_e^\# \mathbf{A} = \begin{bmatrix} 1.00 + j0.00 & -0.02 + j0.18 \\ 0.01 + j0.14 & 1.00 + j0.00 \end{bmatrix}$$

and the global rejection level I_{perf} is reduced to -12.86 dB. The CW distributions of the separated signals are shown in Fig. 9(b).

Fig. 10 shows the CW distributions of the separated signals under the same condition as Fig. 9(a), with the utilization of the spatial averaging method. Again, it is clear that the time-frequency distributions of both cases are the same as the source signals, and $\hat{\mathbf{A}}_e^\# \mathbf{A}$ are exactly an identity matrix. The same results can be obtained when only the autoterm (t, f) points are used.

Fig. 11 shows the global rejection level versus the frequency difference δf between the two chirps, where the input SNR is 20 dB. It is evident from this figure that the kernel method fails when the two signals have close time-frequency signatures.

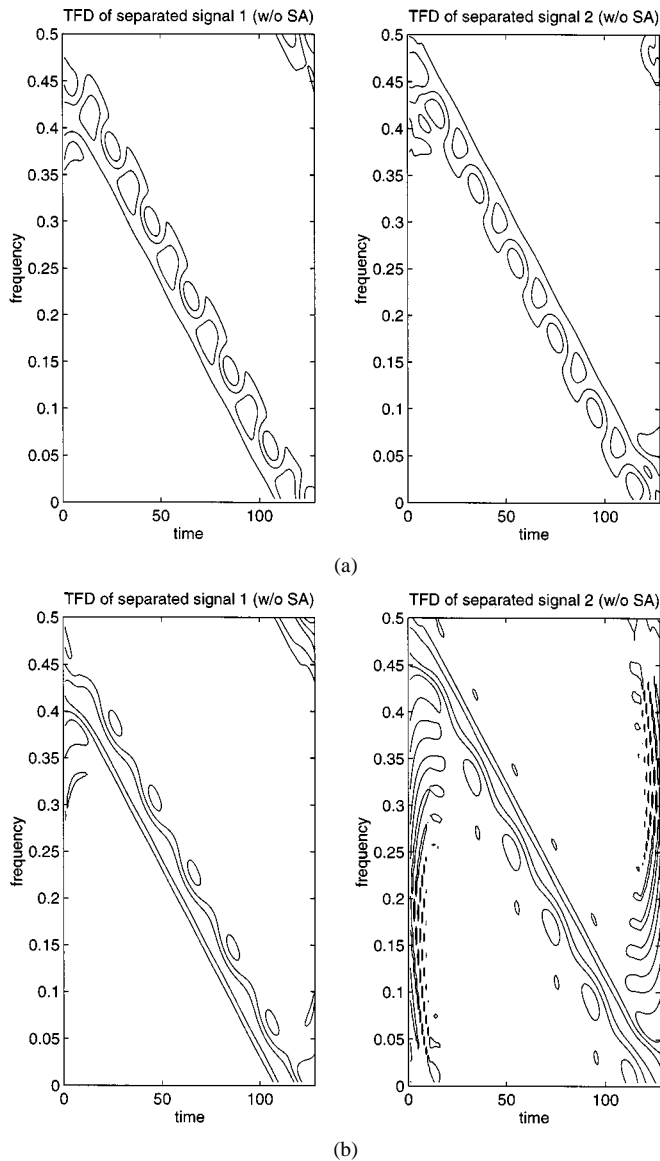


Fig. 9. TFD of the separated signals without spatial averaging (Choi–Williams distribution). (a) Using peak time–frequency points. (b) Using autoterm points.

Using the proposed spatial averaging method outperforms the case when no spatial averaging is applied. Three important observations on the difference between the WV distribution and the CW distribution in the context of source separation are in order. First, the CW kernel effectively reduces the crossterms, particularly when δf is large. Accordingly, crossterms are not as large as the autoterms, and as such, it is unlikely for the crossterms to be selected and incorporated in the joint-diagonalization scheme. Second, when δf is large enough, the global rejection level is significantly reduced for the CW distribution, even when spatial averaging is not applied. Third, when the spatial averaging method is used, the performance at small frequency offset from the CW distribution is worse than that obtained from the WV distribution. The reason is that source separation is perturbed by the presence of noise, and the performance nevertheless is sensitive to the input SNR. When comparing the WV distribution and the CW distribution, the noise floor relative to peak values is lower in the WV distribution than in the CW for the underlying chirp signal example.

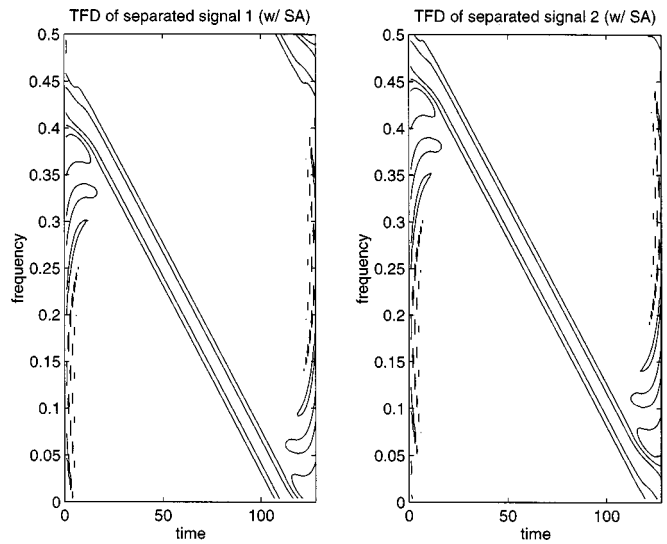


Fig. 10. TFD of the separated signals with spatial averaging (Choi–Williams distribution).

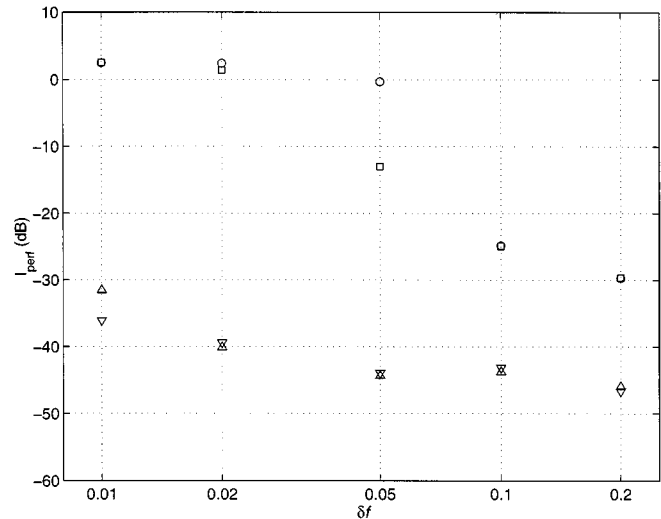


Fig. 11. Global rejection level versus frequency difference δf (Choi–Williams distribution). (Input SNR = 20 dB; \circ : without spatial averaging; \triangle : with spatial averaging; \square : without spatial averaging using autoterm points; ∇ : with spatial averaging using autoterm points).

To show the effect of the input SNR on the source separation performance, Figs. 12 and 13 depict the global rejection level versus the input SNR, where the frequency difference is 0.01. Increasing the SNR certainly improves the source separation performance when spatial averaging is applied. On the other hand, without spatial averaging, the source separation performance holds an almost constant high level. Such a performance demonstrates that crossterms are more of a fundamental problem than noise in TFD-based source-separation problems.

In the second set of simulations, ω is set to zero in (38), rendering the two source signals identical in terms of their instantaneous frequency characteristic. However, one of the two source signals is amplitude modulated, which is caused by a nonzero positive value of α .

Fig. 14 shows the global rejection level versus α , where the WV distribution is considered, and the input SNR is 20 dB. It is clear that the two signals cannot be separated without spatial

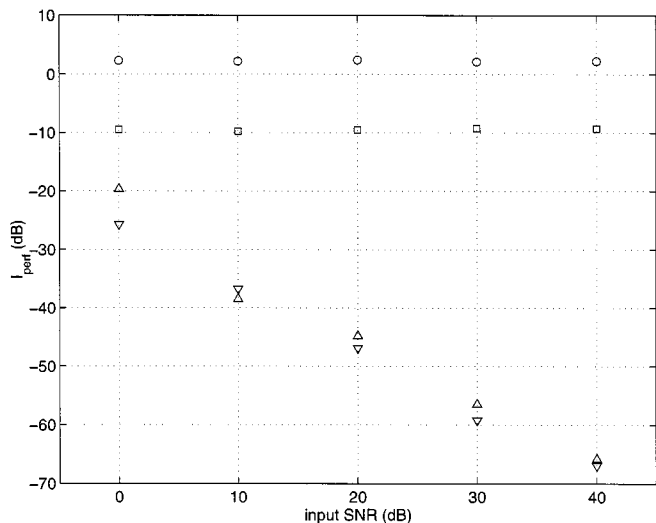


Fig. 12. Global rejection level versus input SNR (Wigner-Ville distribution). ($\delta f = 0.01$; o: without spatial averaging; Δ : with spatial averaging; \square : without spatial averaging using autoterm points; ∇ : with spatial averaging using autoterm points).

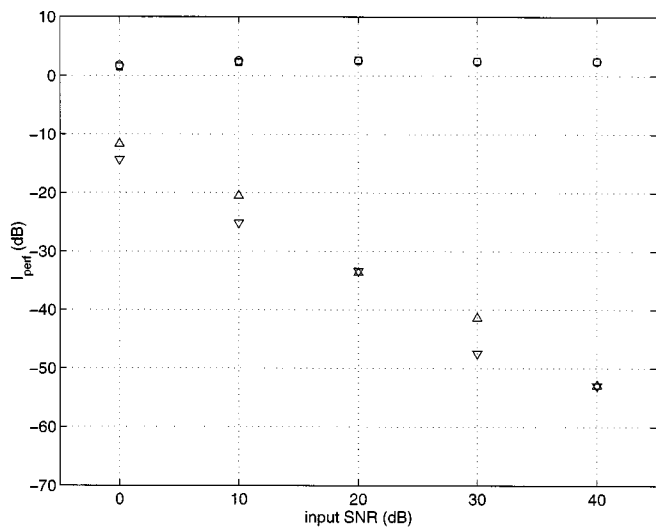


Fig. 13. Global rejection level versus input SNR (Choi-Williams distribution). ($\delta f = 0.01$; o: without spatial averaging; Δ : with spatial averaging; \square : without spatial averaging using autoterm points; ∇ : with spatial averaging using autoterm points).

averaging, but when applying spatial averaging, satisfactory performance of source separation can be achieved. For $\alpha = 0.002$, the proposed technique yields a global rejection level -26.72 dB.

V. CONCLUSIONS

Spatial averaging of spatial time-frequency distributions has been introduced and the role of spatial averaging in mitigating the effects of crossterms when bilinear transforms are used for signal recovery has been shown. The spatial averaging of the spatial time-frequency distributions of the data across an antenna array removes the undesired effect of crossterms between the impinging signals. These terms reside along the off-diagonal entries of the source time-frequency distribution matrix and consequently impede the source separation performance,

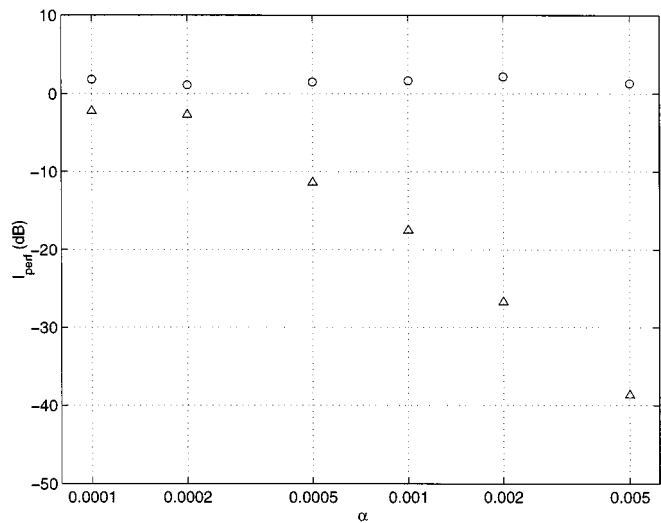


Fig. 14. Global rejection level versus α (Wigner-Ville distribution). (Input SNR = 20 dB; o: without spatial averaging; Δ : with spatial averaging).

which is based on preassumed diagonal matrix structure. Spatial averaging amounts to forming a spatial Hermitian Toeplitz matrix using the auto- and cross-time-frequency distributions of the data over one half of the uniform linear array. This matrix is then added to the spatial matrix corresponding to the other half of the array. The desired effect of this averaging is reallocating the interaction between the source signals in the time-frequency domain from the off-diagonal to the diagonal elements of the source TFD matrix. In this respect, unlike the method proposed in [2], cross-terms, due to their potential high values, are regarded as useful components that could be used for improved performance. Spatial averaging can be applied to all members of Cohen's class of TFDs, irrespective of the employed smoothing kernel. When using a time-frequency kernel, the problem amounts to averaging in all three dimensions of time, frequency, and space.

Joint-diagonalization (JD) is applied to include multiple spatially averaged time-frequency distributions at different time-frequency points. With cross-terms moved to the diagonal entries of the TFD matrix, the prime task of the source separation based on the JD scheme is to avoid degenerate eigenvalues that are responsible for the nonuniqueness solution of the problem.

Simulation examples were presented to illustrate the effectiveness of the new approach. The two performance measures used were the global rejection level and the values of the off-diagonal elements of the product of the mixing matrix and the Pseudo inverse of its estimate. Two sources and five sensors were considered. The source signals were chirp signals with the same sweeping frequency, but their corresponding constant frequencies and amplitudes were offset by different values. Both Wigner-Ville and Choi-Williams distributions were considered. It was shown that the spatial averaging method significantly improves the performance measures over the nonspatially averaging method, specifically when the two signals have close time-frequency signatures.

Without spatial averaging, performance is very sensitive to whether only auto-term or cross-term points or their mix are

incorporated in the source separation procedure. With spatial averaging, this is no longer a concern since both terms appear along the diagonal. It is also shown that the Choi–Williams distribution provides better results than the Wigner–Ville distribution when no spatial averaging is applied since it lowers the likelihood of selecting crossterm points. With spatial averaging, the issue becomes merely SNR, and in this respect, the Wigner–Ville distribution, due to its high peak values, yields better performance than the Choi–Williams distribution. Therefore, the time–frequency smoothing becomes unnecessary whenever spatial array averaging is possible.

REFERENCES

- [1] A. Belouchrani and M. Amin, "Source separation based on the diagonalization of a combined set of spatial time–frequency distribution matrices," in *Proc. ICASSP*, Munich, Germany, Apr. 1997.
- [2] —, "Blind source separation based on time–frequency signal representation," *IEEE Trans. Signal Processing*, vol. 46, pp. 2888–2898, Nov. 1998.
- [3] —, "Blind source separation using joint signal representations," in *Proc. SPIE: Advanced Algorithms Architectures Signal Process.*, San Diego, CA, Aug. 1997.
- [4] M. G. Amin and A. Belouchrani, "Blind source separation using the spatial ambiguity functions," in *Proc. IEEE Int. Symp. Time–Freq. Time–Scale Anal.*, Pittsburgh, PA, Oct. 1998, pp. 413–416.
- [5] A. Belouchrani and M. Amin, "Time–frequency MUSIC," *IEEE Signal Processing Lett.*, vol. 6, pp. 109–110, May 1999.
- [6] S. U. Pillai, *Array Signal Processing*. New York: Springer-Verlag, 1989.
- [7] L. Cohen, *Time–Frequency Analysis*. Englewood Cliffs, NJ: Prentice-Hall, 1995.
- [8] L. Tong, Y. Inouye, and R.-W. Liu, "Waveform-preserving blind estimation of multiple independent sources," *IEEE Trans. Signal Processing*, vol. 41, pp. 2461–2470, July 1993.
- [9] A. Belouchrani, K. A. Meraim, J.-F. Cardoso, and E. Moulines, "A blind source separation techniques using second order statistics," *IEEE Trans. Signal Processing*, vol. 45, pp. 434–444, Feb. 1997.
- [10] H. I. Choi and W. J. Williams, "Improved time–frequency representation of multicomponent signals using exponential kernels," *IEEE Trans. Acoust., Speech, Signal Processing*, vol. 37, pp. 862–871, June 1989.
- [11] P. Stoica and K. Sharman, "Maximum likelihood methods for direction-of-arrival estimation," *IEEE Trans. Acoust., Speech, Signal Processing*, vol. 38, pp. 1132–1143, July 1990.
- [12] Y. Hua and T. K. Sarkar, "Matrix pencil method for estimating parameters of exponentially damped/undamped sinusoids in noise," *IEEE Trans. Acoust., Speech, Signal Processing*, vol. 38, pp. 814–824, May 1990.
- [13] R. O. Schmidt, "Multiple emitter location and signal parameter estimation," *IEEE Trans. Antennas Propagat.*, vol. 34, pp. 276–280, Mar. 1986.
- [14] A. J. Barabell, "Improving the resolution performance of eigenstructure-based direction-finding algorithms," in *Proc. ICASSP*, Boston, MA, 1983, pp. 336–339.
- [15] B. D. Rao and K. V. S. Hari, "Performance analysis of root-MUSIC," *IEEE Trans. Acoust., Speech, Signal Processing*, vol. 37, pp. 1939–1949, Dec. 1989.
- [16] R. Roy and T. Kailath, "ESPRIT—Estimation of signal parameters via rotational invariance techniques," *IEEE Trans. Acoust., Speech, Signal Processing*, vol. 37, pp. 984–995, July 1989.
- [17] Y. Zhang, W. Mu, and M. G. Amin, "Subspace analysis of spatial time–frequency distribution matrices," *IEEE Trans. Signal Processing*, submitted for publication.
- [18] Y. Zhang, W. Mu, and M. G. Amin, "Time–frequency maximum likelihood methods for direction finding," *J. Franklin Inst.*, vol. 337, pp. 483–497, July 2000.
- [19] Y. Zhang and M. G. Amin, "Blind separation of sources based on their time–frequency signatures," in *Proc. ICASSP*, Istanbul, Turkey, June 2000.
- [20] J. E. Evans, J. R. Johnson, and D. F. Sun, "High resolution angular spectrum estimation techniques for terrain scattering analysis and angle of arrival estimation," in *Proc. First Acoust., Speech, Signal Process. Workshop Spectral Estim.*, Hamilton, ON, Canada, Aug. 1981.
- [21] T. J. Shan and T. Kailath, "On spatial smoothing for DOA estimation of coherent sources," *IEEE Trans. Acoust., Speech, Signal Processing*, vol. ASSP-33, pp. 806–811, 1985.
- [22] R. T. Williams, S. Prasad, A. K. Mahalanabis, and L. H. Sibul, "An improved spatial smoothing technique for bearing estimation in multipath environment," *IEEE Trans. Acoust., Speech, Signal Processing*, vol. 36, pp. 425–432, 1988.
- [23] S. U. Pillai and B. H. Kwon, "Forward/backward spatial smoothing techniques for coherent signal identification," *IEEE Trans. Acoust., Speech, Signal Processing*, vol. 37, pp. 8–15, Jan. 1989.
- [24] S. U. Pillai, Y. Barness, and F. Haber, "A new approach to array geometry for improved spatial spectrum estimation," *Proc. IEEE*, vol. 73, pp. 1522–1524, Oct. 1985.



Yimin Zhang (M'88) received the M.S. and Ph.D. degrees from the University of Tsukuba, Tsukuba, Japan, in 1985 and 1988, respectively.

He joined the faculty of the Department of Radio Engineering, Southeast University, Shanghai, China, in 1988. He served as a Technical Manager at Communication Laboratory Japan from 1995 to 1997 and a Visiting Researcher at ATR Adaptive Communications Research Laboratories, Tokyo, Japan, from 1997 to 1998. Currently, he is a Research Fellow with the Department of Electrical

and Computer Engineering, Villanova University, Villanova, PA. His current research interests are in the areas of array signal processing, space-time adaptive processing, blind signal processing, digital mobile communications, and time–frequency analysis.



Moeness G. Amin (SM'91) received the Ph.D. degree in electrical engineering in 1984 from University of Colorado, Boulder.

He has been on the Faculty of the Department of Electrical and Computer Engineering at Villanova University, Villanova, PA, since 1985, where is now a Professor. His current research interests are in the areas of time–frequency analysis, spread spectrum communications, smart antennas, and blind signal processing.

Dr. Amin was an Associate Editor of the IEEE TRANSACTIONS ON SIGNAL PROCESSING from 1995 to 1997 and a Member of the Technical Committee of the IEEE Signal Processing Technical Committee on Signal Processing for Communications. He was the General Chair of the 1994 IEEE International Symposium on Time–Frequency and Time–Scale Analysis. He is the General Chair of the 2000-IEEE Workshop on Statistical Signal and Array Processing. He was the recipient of the 1997 IEEE Philadelphia Section Service Award and the IEEE Third Millennium Medal. He was also the recipient of the 1997 Villanova University Outstanding Faculty Research Award. He serves on the Committee of Arts and Science of the Franklin Institute.